Scientific Research Publishing

Optics and Photonics Journal, 2023, 13, 109-118
https://www.scirp.org/journal/opj
ISSN Online: 2160-889X
ISSN Print: 2160-8881

Numerical Simulation of External-Cavity Distributed Feedback Semiconductor Laser

Tianyu Guan, Chaoze Zhang, Yuqin Mao, Ligang Huang*, Tao Zhu

Key Laboratory of Optoelectronic Technology and Systems, Chongqing University, Chongqing, China
Email: *lghuang@cqu.edu.cn

How to cite this paper: Guan, T.Y., Zhang, C.Z., Mao, Y.Q., Huang, L.G. and Zhu, T. (2023) Numerical Simulation of External-Cavity Distributed Feedback Semiconductor Laser. *Optics and Photonics Journal*, **13**, 109-118.
https://doi.org/10.4236/opj.2023.136009

Received: April 24, 2023
Accepted: June 27, 2023
Published: June 30, 2023

Abstract

We propose a theoretical model to describe external-cavity distributed feedback semiconductor lasers and investigate the impact of the number of external feedback points on linewidth and side-mode suppression ratio through numerical simulation. The simulation results demonstrate that the linewidth of external-cavity semiconductor lasers can be reduced by increasing the external cavity length and feedback ratio, and adding more external feedback points can further narrow the linewidth and enhance the side mode suppression ratio. This research provides insight into the external cavity distributed feedback mechanism and can guide the design of high-performance external cavity semiconductor lasers.

Keywords

External-Cavity Distributed Feedback, Linewidth Compression, Multi-Point Feedback, Narrow-Linewidth Laser, Semiconductor Laser

1. Introduction

In recent years, the demand for high-performance narrow linewidth lasers has been increasing due to their important applications in precision metrology, optical communication, and sensing. Currently, various types of narrow linewidth lasers have been developed, such as distributed feedback (DFB) lasers, distributed Bragg reflector (DBR) lasers, external-cavity semiconductor lasers (ECSLs), and fiber lasers. Among them, ECSLs are considered to be a promising platform for achieving narrow linewidths and high side mode suppression ratio (SMSR). Researchers have been exploring various techniques to further optimize the performance of ECSLs, such as incorporating frequency-selective elements into the external cavity [1]-[6]. These efforts have led to the demonstration of ECSLs with sub-kHz linewidths and SMSR exceeding 65 dB [7]. However, the external

feedback generated by single external cavity will cause periodic laser phase hopping as the main cavity laser interferes with the feedback light, which eventually causes the laser to oscillate into multiple new longitudinal modes. Thus, the research on narrow linewidth lasers is still ongoing to further improve their performance and address the existing challenges.

Based on breaking through the limitations of single external cavity feedback, our research group proposes a narrow linewidth laser model assisted by external-cavity distributed feedback [8] [9] [10]. In 2014, we combined the distributed feedback structure with a stable laser main resonator, resulting in a fiber laser with a linewidth of 130 Hz [11]. Additionally, we applied the distributed feedback mechanism to dual-wavelength tunable lasers to achieve simultaneous compression of different wavelength lasers [12] [13] [14]. In 2022, we constructed a fiber laser system with a multi-longitudinal mode main cavity and a distributed feedback structure, producing an ultra-narrow linewidth laser output with a side-mode suppression ratio of 70 dB and a wavelength tuning range of 40 nm [15]. In order to further achieve the ultimate compression of the laser linewidth, we built a hybrid integrated on-chip laser system with a single longitudinal mode DFB main cavity combined with a distributed feedback structure [16]. Eventually, the experimental system obtained a laser output with an integrated linewidth of 10 Hz under normal conditions. Although the external cavity distributed feedback model has shown great promise in experiments, the theoretical model requires further exploration to fully describe the influence of the external-cavity distribution feedback mechanism on the external cavity semiconductor lasers. Such an understanding would provide a necessary theoretical foundation to guide the further development of external cavity distributed feedback semiconductor lasers.

In this work, we propose a mathematical model to describe external-cavity distributed feedback semiconductor lasers and analyze the impact of the number of external feedback cavities on the laser linewidth and side-mode suppression ratio. We also report on the effects of external cavity length and feedback ratio on external-cavity distributed feedback semiconductor lasers, which can help understand the feedback mechanisms of the external-cavity semiconductor lasers.

2. Theory

We propose a theoretical model of calculating distributed feedback external cavity semiconductor lasers, as shown in **Figure 1**. The structure consists of single longitudinal mode laser and a set of randomly distributed feedback points, each with the same feedback ratio. The distance between each feedback point and the output port of the laser is $L_{ext(i)}$.

According to [17] [18], at medium feedback level, the photon number S, phase φ and the carrier concentration n of the external-cavity semiconductor lasers with multi-cavity feedback points can be further derived by the Lang-Kobayashi laser rate equation as

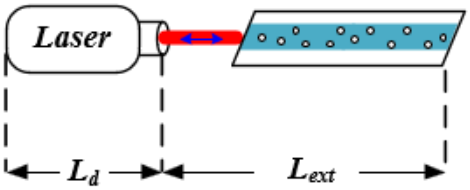

Figure 1. Schematic diagram of the external-cavity laser.

$$\frac{dS}{dt}=\left(g(n,S)-\frac{1}{\tau_p}\right)+Q+2k_c\sqrt{S_\tau(t)S(t)}\cos(\varphi(t)-\varphi_\tau(t))+F_s(t) \tag{1}$$

$$\frac{d\varphi}{dt}=\frac{1}{2}\alpha G(n-n_{th})-k_c\sqrt{\frac{S_\tau(t)}{S(t)}}\sin(\varphi(t)-\varphi_\tau(t))+F_\varphi(t) \tag{2}$$

$$\frac{dn}{dt}=\frac{I}{e}-\frac{n}{\tau_s}-g(n,S)S+F_n(t) \tag{3}$$

τ_p is the photon lifetime, τ_s is the carrier lifetime, f_{ext} is the power fraction of light returned to the cavity, α is the linewidth enhancement factor, ω_0 is the center frequency of the semiconductor lasers without feedback, n_{th} is the number of non-equilibrium carriers at the generation threshold, I is the pump current, e is the electron charge. $\sqrt{S_\tau(t)}$ is the modulus of the total feedback complex electric field, and $S_\tau(t)$ is the total feedback intensity. $\varphi_\tau(t)$ is the phase of the total feedback complex electric field. The total feedback complex electric field, which is denoted by $\tilde{A}(t)$, can be expressed as:

$$\tilde{A}(t)=\sum_{i=1}^{N}\sqrt{S(t-\tau_i)}\exp(j\varphi(t-\tau_i)) \tag{4}$$

where N is the quantity of feedback points, $S(t-\tau_i)$ is the light intensity from each feedback point with the ordinal number of i and the roundtrip delay time of τ_i, and $\varphi(t-\tau_i)$ is the light phase from each feedback point. F_s, F_φ and F_n are the Langevin noise with Gaussian distribution simulated by random number. k_c is the reflection coefficient of the semiconductor laser, which can be expressed as

$$k_c=\frac{1}{\tau_d}\frac{1-R}{\sqrt{R}}\sqrt{f_{ext}} \tag{5}$$

where R is the reflection coefficient of the main cavity of the semiconductor laser, $\tau_d=2\eta L_d/c$ is the round-trip time of the main cavity of the laser, η is the refractive index of the laser main cavity, L_d is the length of the main cavity, c is the speed of light in vacuum. The spontaneous emissivity Q can be expressed as:

$$Q=\frac{n_{sp}}{\tau_p}\left(\frac{2(1-R)}{\sqrt{R}\ln\left(\frac{1}{R^2}\right)}\right)^2 \tag{6}$$

where n_{sp} is the inversion coefficient of semiconductor laser. $G(n, S)$ is the gain, which can be expressed as

$$g(n,S)=\frac{G(n-n_0)}{(1+\frac{S}{S_n})} \tag{7}$$

where S_n corresponds to the photon number at the threshold, $G(n - n_0)$ is the differential gain and n_0 is the number of non-equilibrium carriers corresponding to zero amplification. The above parameters describe the classical external cavity semiconductor laser and simulation values are listed in **Table 1**.

3. Simulation and Discussion

We utilize the fourth-order Runge-Kutta method to conduct numerical simulations of the rate equation for the laser. The carrier numbers nth and Sn are determined based on the analytical solution for a semiconductor laser that operates in steady-state isolation. The complex amplitude-based Fourier transform is employed to reconstruct the laser spectrum based on the obtained photon number, phase, and carrier number. External feedback is a common method to narrow the linewidth of a laser. However, excessive external feedback can lead to the emergence of multi-longitudinal modes, resulting in feedback peaks in the frequency noise spectrum. Multi-point distributed feedback can alleviate this issue by further compressing the linewidth and weakening the mode oscillation induced by external feedback. This allows the laser to re-evolve into a single longitudinal mode, thus achieving a narrow linewidth output.

Based on the reconstructed frequency noise spectrum, we can obtain the intrinsic linewidth. **Figure 2** shows the changes of intrinsic linewidth of external-cavity distributed feedback semiconductor lasers under different external-cavity feedback numbers. We used a fixed feedback ratio of 1×10^{-5}, a longest cavity length of 10 m, and a variable cavity length between 4.49 m to 4.51 m. The lengths of other feedback cavities were chosen randomly between 0 - 10 m. To ensure stable operation of the semiconductor laser without feedback, we executed the program 5×10^6 times with a step size of 10 ps. For the feedback case,

Table 1. Laser parameters.

Symbol	Quantity	Value
L_d	Semiconductot cavity length	1000 μm
η	Semiconductor cavity refractive index	3.6
R	Reflection of the rear semiconductor laser cavity mirror	0.32
τ_s	Carrier lifetime	2 ns
τ_p	Photon lifetime	20 ps
n_0	Carrirer number to reach zero again	2×10^8
G	$(=dg/dn)$	8×10^{-2} s^{-1}
n_{sp}	Inversion factor	3
α	Linewidth enhancement factor	3

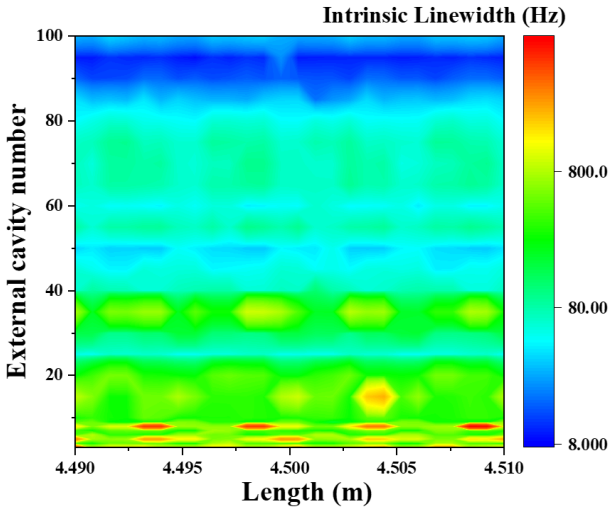

Figure 2. The intrinsic linewidth evolution with multi external-cavity distributed feedback.

the program was run 1.5×10^7 times to ensure complete evolution of the external cavity semiconductor laser. It can be seen that as the number of external cavity feedback points increases, the laser's intrinsic linewidth gradually decreases from the 1×10^3 level to the 1×10^1 level. This suggests that the addition of more external cavity feedback points can effectively compress the linewidth of the external-cavity semiconductor laser.

The SMSR of a single external-cavity semiconductor laser varies with the length of the external cavity. When the external cavity feedback is weak, the side mode introduced by the external cavity feedback will gradually strengthen and compete with the main mode, leading to a decline in the side mode suppression ratio. To improve this, multi external cavity distributed feedback can be introduced. **Figure 3** shows the changes in the side mode suppression ratio of the external cavity distributed feedback semiconductor laser. As the number of external cavity feedback points increases, the side mode suppression ratio of the laser steadily increases. With more than 90 external cavity points, the SMSR reaches 70 dB, while the intrinsic linewidth of the laser narrows to the level of 10 Hz. This indicates that external cavity distributed feedback can effectively narrow the linewidth and improve the side mode suppression ratio of the laser.

Figure 4 shows the spectrum and frequency noise spectrum of the laser with different external cavity feedback numbers, which more clearly illustrates the changes of the above-mentioned intrinsic linewidth and SMSR. **Figures 4(a)-(c)** shows the reconstructed laser spectra when the external cavity feedback points are 3, 50, and 100 respectively. By increasing the number of external cavity points, the side mode introduced by the weak external cavity feedback is continuously suppressed, and the SMSR is continuously increased from 50 dB to 70 dB. Suppression of multi-longitudinal modes can also be shown in the frequency noise spectrum. It can be seen from **Figures 4(d)-(f)** that there has high-frequency noise peak in the frequency range from 10 MHz to 100 MHz, but this high-

frequency noise peak is continuously sup-pressed as the number of external cavity points increases. It is worth noting that while the frequency noise in the frequency range below 1 MHz can be reduced from 10^3 Hz^2/Hz to the level of 10^1 Hz^2/Hz, the effect of frequency noise reduction is gradually weakened for higher frequency noise. There is no significant difference in the frequency noise above 100 MHz between different external cavity lasers under different numbers of cavity points. This suggests that increasing the number of external cavity points cannot effectively compress the frequency noise of the high frequency span.

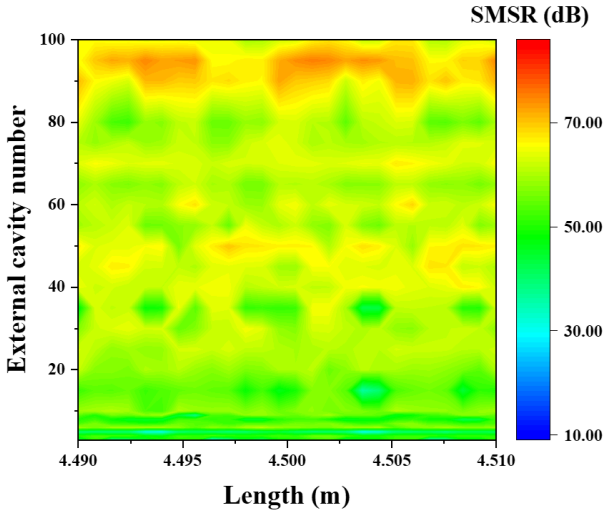

Figure 3. The SMSR evolution with multi external-cavity distributed feedback.

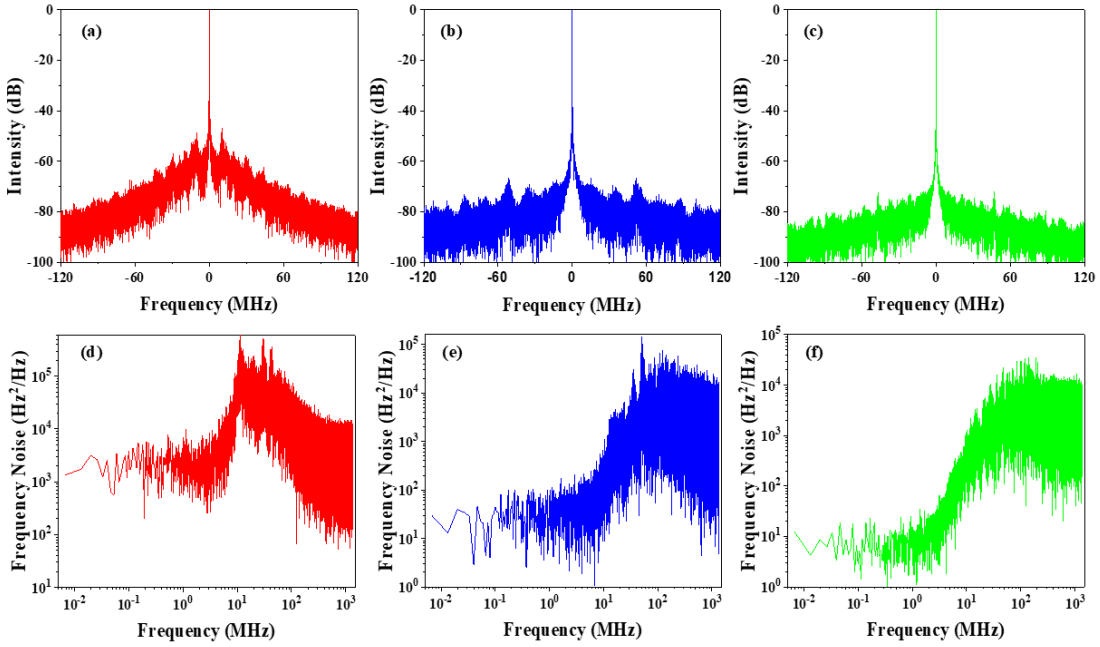

Figure 4. The frequency noise and spectrum evolution with multi external-cavity distributed feedback. (a) The reconstructed laser spectra with 3 external-cavity feedback. (b) The reconstructed laser spectra with 50 external-cavity feedback. (c) The reconstructed laser spectra with 100 external-cavity feedback. (d)-(f) Typical frequency noise spectrum with 3, 50 and 100 external-cavity feedback.

Previous studies have demonstrated that under single-point feedback, the linewidth of a laser increases as the feedback ratio and the length of the external cavity are increased [19]. Our research has confirmed that this mechanism remains valid for multi-point distributed feedback. As shown in **Figure 5**, we maintain a fixed feedback ratio of 1×10^{-5} for each feedback point and vary the length of the longest cavity to 1 m and 100 m, respectively, while proportionally increasing the lengths of the other external cavities. The intrinsic linewidth of the laser decreases as the length of the external cavity increases, and increasing the number of external cavity points can further reduce the linewidth. These observations are consistent with the conclusions drawn for single-point feedback.

Figure 6 shows the effect of increasing the feedback ratio while keeping the longest external cavity length fixed at 10 m. It can be observed that, as the feedback ratio increases to the order of 1×10^{-4}, the linewidth of the laser continues to decrease, which is consistent with previous research results. It is worth noting that the intrinsic linewidth of the laser cannot be further reduced and tends to

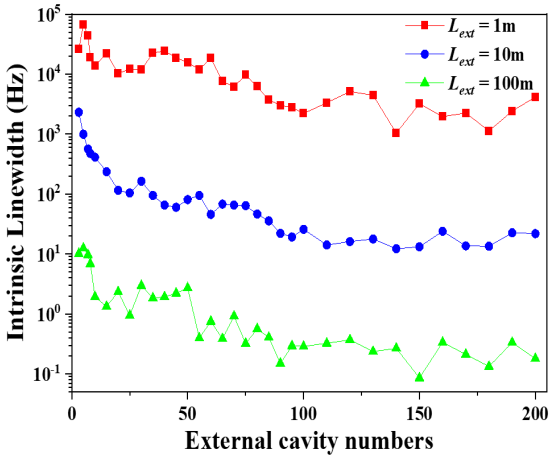

Figure 5. The influence of the maximum external-cavity length on intrinsic linewidth with a fixed feedback ratio of 10^{-5}.

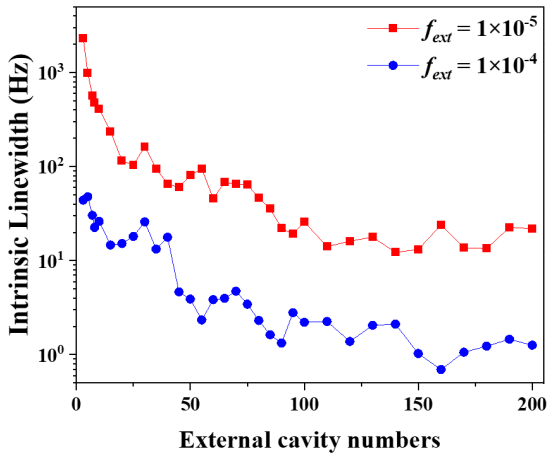

Figure 6. The influence of the feedback ratio on intrinsic linewidth with a fixed maximum external-cavity length.

fluctuate within a certain range when the number of external cavity feedback points exceeds a certain value (100 points). However, the increase in the number of external cavity feedback points will inevitably increase the cost of the external cavity semiconductor laser. Therefore, it is necessary to strike a balance between the number of external cavities and performance to realize high-performance external cavity semiconductor laser at a reasonable cost.

4. Conclusions

We demonstrate a model for analyzing external-cavity distributed feedback semiconductor lasers. The results indicate that increasing the number of external cavity feedback points to achieve distributed feedback can further optimize the performance of the external cavity semiconductor laser. When the feedback ratio and the maximum external cavity length are determined, by increasing the number of feedback points, the side mode suppression ratio can be improved while narrowing the linewidth. When the number of external cavity points reaches a certain number, continuing to increase the feedback points cannot continue to narrow the linewidth, but fluctuates within a certain range.

It is important to note that in this model, the feedback ratio for each feedback point is fixed, meaning that increasing the number of external cavity points, increasing the length of the external cavity, or increasing the single-point feedback ratio all result in an increase in the amount of external feedback received by the main cavity. In accordance with classical external-cavity semiconductor laser theory, when the amount of feedback falls within a certain range, increasing the amount of feedback can continuously narrow the linewidth of the laser, but can also introduce new longitudinal modes into the main cavity. The use of external cavity distributed feedback can effectively suppress the multi-longitudinal mode oscillation introduced by the external cavity feedback, and enable single longitudinal mode operation during the linewidth compression process.

The theoretical analysis and simulation of intrinsic linewidth and SMSR of external cavity distributed semiconductor lasers will help to deepen the understanding of external cavity distributed feedback mechanism, and can also guide the design of narrow linewidth semiconductor lasers with high SMSR.

Conflicts of Interest

The authors declare no conflicts of interest regarding the publication of this paper.

References

[1] Ding, K., Ma, Y., Wei, L., Li, X., Shi, J., Li, Z., Qu, Y., Li, L., Qiao, Z. and Liu, G. (2022) Research on Narrow Linewidth External Cavity Semiconductor Lasers. *Crystals*, **12**, 956. https://doi.org/10.3390/cryst12070956

[2] Fischer, A., Yousefi, M., Lenstra, D., Carter, M.W. and Vemuri, G. (2004) Experimental and Theoretical Study of Semiconductor Laser Dynamics due to Filtered Optical Feedback *IEEE Journal of Selected Topics in Quantum Electronics*, **10**, 944-

954. https://doi.org/10.1109/JSTQE.2004.835997

[3] Huang, B., Shu, X. and Du, Y. (2017) Intensity Modulated Torsion Sensor Based on Optical Fiber Reflective Lyot Filter. *Optics Express*, **25**, 5081-5090. https://doi.org/10.1364/OE.25.005081

[4] Jelger, P. and Laurell, F. (2007) Efficient Narrow-Linewidth Volume-Bragg Grating-Locked Nd: Fiber Laser. *Optics Express*, **15**, 11336-11340. https://doi.org/10.1364/OE.15.011336

[5] Zheng, J., Zhang, Y., Li, L., Tang, S., Sh, Y. and Chen, X. (2015) An Equivalent-Stepped-Index-Coupled DFB Semiconductor Laser and Laser Array Realized by Stepping the Duty Cycle of the Sampled Bragg Grating *Optics & Laser Technology*, **67**, 38-43. https://doi.org/10.1016/j.optlastec.2014.09.011

[6] Li, F., Lan, T., Huang, L., Ikechukwu, I.P., Liu, W. and Zhu, T. (2019) Spectrum Evolution of Rayleigh Backscattering in One-Dimensional Waveguide. *Opto-Electronic Advances*, **2**, 08190012. https://doi.org/10.29026/oea.2019.190012

[7] Wang, Y., Wu, H., Chen, C., Zhou, Y., Wang, Y., Liang, L., Tian, Z., Qin, L. and Wang, L. (2019) An Ultra-High-SMSR External-Cavity Diode Laser with a Wide Tunable Range around 1550 nm. *Applied Sciences*, **9**, 4390. https://doi.org/10.3390/app9204390

[8] Zhu, T., Bao, X. and Chen, L. (2011) A Single Longitudinal-Mode Tunable Fiber Ring Laser Based on Stimulated Rayleigh Scattering in a Nonuniform Optical Fiber. *Journal of Lightwave Technology*, **29**, 1802-1807. https://doi.org/10.1109/JLT.2011.2142292

[9] Zhu, T., Bao, X. and Chen, L. (2012) A Self-Gain Random Distributed Feedback Fiber Laser Based on Stimulated Rayleigh Scattering. *Optics Communications*, **285**, 1371-1374. https://doi.org/10.1016/j.optcom.2011.11.072

[10] Zhu, T., Bao, X., Chen, L., Liang, H. and Dong, Y. (2010) Experimental Study on Stimulated Rayleigh Scattering in Optical Fibers. *Optics Express*, **18**, 22958-22963. https://doi.org/10.1364/OE.18.022958

[11] Zhu, T., Huang, S., Shi, L., Huang, W., Liu, M. and Chiang, K. (2014) Rayleigh Backscattering: A Method to Highly Compress Laser Linewidth. *Chinese Science Bulletin*, **59**, 4631-4636. https://doi.org/10.1007/s11434-014-0603-0

[12] Huang, S., Zhu, T., Cao, Z., Liu, M., Deng, M., Liu, J. and Li, X. (2016) Laser Linewidth Measurement Based on Amplitude Difference Comparison of Coherent Envelope. *IEEE Photonics Technology Letters*, **28**, 759-762. https://doi.org/10.1109/LPT.2015.2513098

[13] Li, Y., Huang, L., Gao, L., Lan, T., Cao, Y., Ikechukwu, I.P., Shi, L., Liu, Y., Li, F. and Zhu, T. (2018) Optically Controlled Tunable Ultra-Narrow Linewidth Fiber Laser with Rayleigh Backscattering and Saturable Absorption Ring *Optics Express*, **26**, 26896-26906. https://doi.org/10.1364/OE.26.026896

[14] Dang, L., Huang, L., Li, Y., Cao, Y., Lan, T., Iroegbu, P.I., Cao, Z., Mei, K., Liang, L. and Fu, S. (2022) A Longitude-Purification Mechanism for Tunable Fiber Laser Based on Distributed Feedback. *Journal of Lightwave Technology*, **40**, 206-214. https://doi.org/10.1109/JLT.2021.3118841

[15] Dang, L., Huang, L., Cao, Y., Li, Y., Iroegbu, P.I., Lan, T., Shi, L., Yin, G. and Zhu, T. (2022) Side Mode Suppression of SOA Fiber Hybrid Laser Based on Distributed Self-Injection Feedback. *Optics & Laser Technology*, **147**, Article 107619. https://doi.org/10.1016/j.optlastec.2021.107619

[16] Dang, L., Huang, L., Shi, L., Li, F., Yin, G., Gao, L., Lan, T., Li, Y., Jiang, L. and Zhu, T. (2023) Ultra-High Spectral Purity Laser Derived from Weak External Distributed

Perturbation. *Opto-Electronic Advances*, **6**, 1-10. https://doi.org/10.29026/oea.2023.210149

[17] Schunk, N. and Petermann, K. (1986) Noise Analysis of Injection-Locked Semiconductor Injection Lasers. *IEEE Journal of Quantum Electronics*, **22**, 642-650. https://doi.org/10.1109/JQE.1986.1073018

[18] Schunk, N. and Petermann, K. (1988) Numerical Analysis of the Feedback Regimes for a Single-Mode Semiconductor Laser with External Feedback. *IEEE Journal of Quantum Electronics*, **24**, 1242-1247. https://doi.org/10.1109/3.960

[19] Guo, W., Tan, M., Jiao, J., Guo, X. and Sun, N. (2014) 980 nm Fiber Grating External Cavity Semiconductor Lasers with High Side Mode Suppression Ratio and High Stable Frequency. *Journal of Semiconductors*, **35**, Article 084007. https://doi.org/10.1088/1674-4926/35/8/084007